

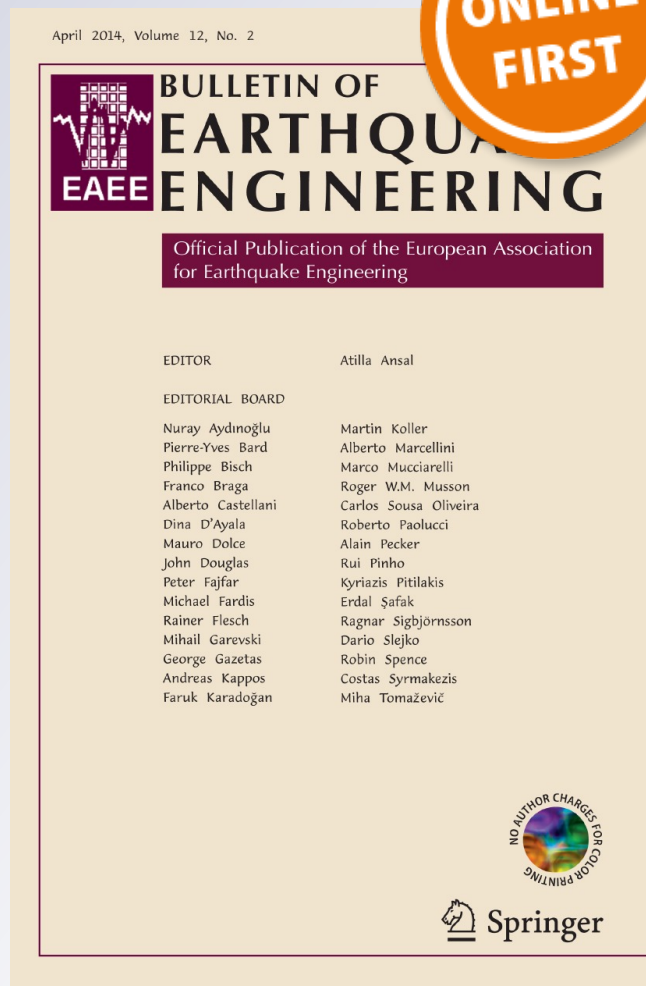
Strong-motion observations from the OGS temporary seismic network during the 2012 Emilia sequence in northern Italy

**Carla Barnaba, Giovanna Laurenzano,
Luca Moratto, Monica Sugan,
Alessandro Vuan, Enrico Priolo, Marco
Romanelli & Paolo Di Bartolomeo**

Bulletin of Earthquake Engineering
Official Publication of the European
Association for Earthquake Engineering

ISSN 1570-761X

Bull Earthquake Eng
DOI 10.1007/s10518-014-9610-4



Your article is protected by copyright and all rights are held exclusively by Springer Science +Business Media Dordrecht. This e-offprint is for personal use only and shall not be self-archived in electronic repositories. If you wish to self-archive your article, please use the accepted manuscript version for posting on your own website. You may further deposit the accepted manuscript version in any repository, provided it is only made publicly available 12 months after official publication or later and provided acknowledgement is given to the original source of publication and a link is inserted to the published article on Springer's website. The link must be accompanied by the following text: "The final publication is available at link.springer.com".

Strong-motion observations from the OGS temporary seismic network during the 2012 Emilia sequence in northern Italy

Carla Barnaba · Giovanna Laurenzano · Luca Moratto ·
Monica Sukan · Alessandro Vuan · Enrico Priolo ·
Marco Romanelli · Paolo Di Bartolomeo

Received: 19 April 2013 / Accepted: 17 March 2014
© Springer Science+Business Media Dordrecht 2014

Abstract Strong-motion data consisting of peak ground acceleration and velocity and 5% damped response spectra are presented for 46 earthquakes of the Emilia seismic sequence which occurred in the Po Plain (northern Italy) in 2012. The data were recorded by the OGS temporary network installed close to the town of Ferrara following the main shock of May 20, 2012. Ground-motion peak parameters and spectral responses are compared with the ground-motion prediction equation (GMPE) of Bindi et al. (Bull Earthq Eng 9:1899–1920, 2011) for soft soils and reverse faults. Peak ground accelerations are in general in good agreement with those predicted by GMPE, while predicted peak ground velocities underestimate the observed data, especially for stronger events at more distant stations. The response spectra follow the trend in peak ground velocities, with observed values higher than predicted values at longer periods. This behavior has been interpreted as a site effect due to the deep soft alluvial cover of the Po Plain, which promotes ground motion characterized by a large low-frequency spectral content that is not yet well modeled by the Italian GMPE. A peculiar behavior was shown by the event occurring on June 6, 04:08:33 UTC, $M = 4.5$, located at the eastern edge of the Po Plain, which produced peak ground accelerations exceeding three times the values estimated by attenuation laws. Such a great discrepancy could be related to post-critically reflected S-waves and multiples from the Moho (SmSM).

Keywords Strong-motion data · Emilia 2012 earthquake · Moho

1 Introduction

On May 20, 2012, at 02:03:53 UTC, the area of Emilia in the Po Plain (northern Italy) was struck by an earthquake of magnitude $M_L 5.9$, with its epicenter located a few kilometers from the towns of Mirandola, Finale Emilia, Bondeno and about 30 km west of the major city of Ferrara (Fig. 1). The seismic sequence included six earthquakes with magnitudes larger

C. Barnaba (✉) · G. Laurenzano · L. Moratto · M. Sukan · A. Vuan · E. Priolo ·
M. Romanelli · P. Di Bartolomeo
OGS, Trieste, Italy
e-mail: cbarnaba@inogs.it

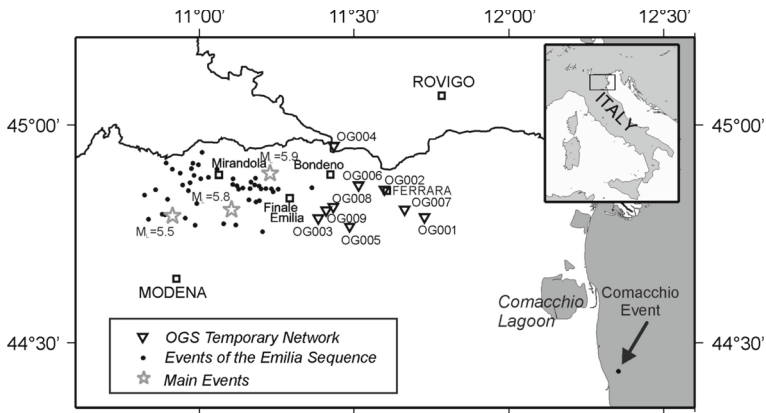


Fig. 1 Location map of the events examined in this study (*black dots*); main events of the Emilia sequence (*grey stars*) are plotted according to the location and local magnitude taken from the OGS Bulletin. *Inverted triangles* are the stations of the temporary OGS network shown in Table 1. The main towns of the area and the Comacchio event are also plotted (see text for more details)

than 5.0 (Scognamiglio et al. 2012), with the largest (ML 5.8) occurring on May 29, 2012 at 07:00:03 UTC and located nearly 12 km WSW of the main shock. The whole sequence involved a delineated 50-km-long strip, 10–15 km wide, elongated in the EW direction, and at 10–15 km depth (Scognamiglio et al. 2012; Malagnini et al. 2012).

The seismic sequence was located within the frontal sector of the northern Apennines, specifically in the buried front of the Ferrara northward-verging active thrust fault belt (Fantoni and Franciosi 2010). In the past, this area has been struck by several events of magnitude ca. 5.5 occurring near Ferrara (1346, 1561) and in the areas of Finale Emilia-Bondeno (1574, 1908, 1986). The most relevant historically known local event is, however, the so-called Ferrara earthquake of 1570 (MW 5.5, Rovida et al. 2011), which was actually a complex seismic sequence, with four strong shocks that caused severe structural damage and partial collapses in Ferrara and its surroundings (Castelli et al. 2012).

According to the present-day seismic hazard classification, this area is characterized by an expected horizontal peak ground acceleration (PGA) with a 10 % probability of being exceeded in 50 years ranging between 0.10 and 0.15 g, which is a moderate level of seismic hazard in Italy (MPS04; <http://zonesismiche.mi.ingv.it>; Stucchi et al. 2011). These values are typical of rocky soil and do not take into account specific site effects. Meletti et al. (2012) analyzed the possibility that the current seismic hazard map is not correct and underestimates the observed data for main shocks. According to Meletti et al. (2012), the highest recorded PGA for the May 29, 2012 event was consistent with seismic hazard estimates, while the response spectra (5 % damped) compared with the design code spectra corrected for soil type (soft soil) as prescribed by the current Italian building code (Norme tecniche per le Costruzioni 2008 (NTC08)) exceeded the code spectrum for 475 years and were much closer to the expected values for 2,475 years. In particular, there was a strong variation between the two horizontal components: the EW component lies below the 2475-year design spectrum, while the NS component exceeds it in several period ranges. This observation could be due to the site effects for longer periods exhibited in many sites within the Po Plain (Bordoni et al. 2012).

The day after the main shock, the Istituto Nazionale di Oceanografia e di Geofisica Sperimentale (OGS) deployed a temporary seismographic network in the Ferrara area (Priolo et al. 2012). The aim of the network was to extend the seismic monitoring area eastward of the

main event location, including some sites that experienced strong evidence of liquefaction phenomena, to evaluate the seismic response at the instrumented sites. All the investigated locations were set on soft soils with low S-wave velocity profiles as determined by the ESAC method from passive noise measurements, corresponding to cohesionless sandy and silty-sandy deposits of the alluvial plain. The preliminary analysis performed by Priolo et al. (2012) on ambient noise as a function of horizontal-to-vertical spectral ratio (HVSR) found common features for all the sites, with a clear amplification peak in the 0.8–1.0 Hz frequency band. This amplification is a common phenomenon in the area between Modena and the mouth of the Po River (Martelli et al. 2011) and has been interpreted as evidence of a stratigraphic boundary between the quaternary alluvium and the Miocene flysch units located at a depth of 130 m (Cocco et al. 2001).

In this research, ground-motion parameters were extracted for 46 earthquakes with magnitude greater than 3.6. The results were compared with the values predicted using the ground-motion prediction equation (GMPE) proposed by Bindi et al. (2011) (hereafter BII1). This GMPE estimates peak ground acceleration (PGA), peak ground velocity (PGV), and 5% damped response spectra (SA) based on the strong-motion database for Italy for a wide set of magnitude and distance ranges.

2 Temporary network and data processing

The OGS temporary network (Fig. 1), consisting of eight stations equipped with velocimetric and accelerometric sensors, was deployed on May 21, 2012, the day after the main shock. A ninth site was set up one month later, on June 25, 2012, as a replacement for a no-longer-available site (OG003). Recording ended for all stations on July 25, 2012.

All the instrumented sites can be classified as soft soil ($V_s < 360$ m/s; Priolo et al. 2012). Two sites were set up east of downtown Ferrara: OG001 in the new city hospital at Cona and OG007 in Aguscello village. Site OG002 was in Ferrara municipality, in front of the chemical-industry district. OG003 and OG009 were set up near sites with moderate and strong liquefaction phenomena in the towns of Sant'Agostino and San Carlo. OG005, OG006, and OG008 were set up in the towns of Poggio Renatico, Vigarano Pieve, and Mirabello, which suffered damage that was moderate, but more severe than neighboring villages according to the macroseismic survey (Tertulliani et al. 2012), taking into account the cumulative effects of the May 20 main shock and its aftershocks, including the strongest events of May 29. OG004 was deployed in Ficarolo village, north of the seismic sequence events. Details on the OGS sites and the instruments used are summarized in Table 1. More information on the temporary network can be found in the OGS Archive System of Instrumental Seismology (OASIS; <http://oasis.crs.inogs.it>) under network code ZR; for each site, monographs giving a geological and geotechnical description of the recording site are available. The continuous stream of recorded data is archived there, and any piece of waveform can be downloaded. The beta version (<http://oasis.crs.inogs.it>) of the OASIS Web page will include the extracted waveforms of the main events as well as the strong-motion parameters, which will be usable as search keys in the ITACA database (Pacor et al. 2011).

To obtain a homogeneous dataset from the recorded velocity and acceleration time series, the data were processed by removal of means and trends, instrument correction with poles and zeroes to obtain displacement time series, bandpass filtering between 0.2 and 45 Hz, and simple and double differentiation to obtain velocity and acceleration time series.

The events analyzed are listed in Table 2. The OGS bulletin was used to fix the event origin time and location (OGS 2013), except for the event occurring on June 6, 2012, at

Table 1 Details of the OGS temporary network

Code	Site	Start	Stop	Lat (°N)	Long (°E)	Sensor type
OG001	Cona-Ospedale Nuovo	2012-05-21	2012-07-25	44.80031	11.69558	Vel
OG002	Comune Ferrara—LLPP	2012-05-21	2012-07-25	44.85249	11.59847	Vel
OG003	Sant'Agostino	2012-05-21	2012-06-25	44.78610	11.38337	Acc
OG004	Ficarolo	2012-05-21	2012-07-25	44.95204	11.43388	Vel
OG005	Poggio Renatico	2012-05-21	2012-07-25	44.76698	11.48494	Vel
OG006	Vigarano Pieve	2012-05-21	2012-07-25	44.86194	11.51468	Vel
OG007	Aguscello	2012-05-21	2012-07-25	44.80652	11.66372	Vel
OG008	Mirabello	2012-05-21	2012-07-25	44.81267	11.43186	Vel
OG009	San Carlo	2012-06-25	2012-07-25	44.80440	11.40893	Acc

More details are available on the Web at <http://oasis.crs.inogs.it>

Table 2 List of the main events ($M_I > 3.6$ in the OGS Bulletin; for event *, the parameters follow the preliminary ISIde Database) analyzed in this study and recorded by the OGS temporary network between 2012/05/21 and 2012/07/23

Date	Time (UTC)	Lat (°)	Long (°)	Depth (km)	M	Ref. Figs. 3 and 4	OG0*								
							01	02	03	04	05	06	07	08	
2012-05-21	16:37:31	44.8562	11.3627	15.4	4.5	b			X						X
2012-05-21	18:02:26	44.8602	11.1918	17.5	3.8										
2012-05-21	18:35:34	44.8540	11.2142	17.6	3.8										
2012-05-22	06:11:15	44.8767	11.1083	14.2	4.0	a			X	X			X	X	X
2012-05-22	09:31:14	44.8538	11.2317	17.5	4.0	a			X	X			X	X	
2012-05-23	06:51:52	44.8530	11.2537	13.5	3.7										
2012-05-23	21:41:18	44.8467	11.2373	15.3	4.4	b			X	X				X	X
2012-05-24	06:26:07	44.8285	11.1593	16.0	3.8										
2012-05-25	10:31:23	44.8238	11.1822	15.2	4.3										
2012-05-25	12:45:01	44.8608	11.1205	15.9	3.7										
2012-05-25	13:14:05	44.8557	11.1402	14.2	4.1	a			X	X				X	X
2012-05-25	13:54:10	44.7708	11.1172	13.8	3.8										
2012-05-26	05:51:16	44.8265	11.1935	16.3	3.8										
2012-05-26	21:07:31	44.7553	11.2033	14.9	4.1	a	X	X	X	X	X	X	X	X	X
2012-05-27	18:18:44	44.7737	11.0780	17.7	4.4	b	X	X	X	X	X	X	X	X	X
2012-05-27	20:25:42	44.8542	11.1630	16.7	4.1	a	X	X	X	X	X	X	X	X	X
2012-05-28	21:27:47	44.8693	11.1662	15.5	3.5										
2012-05-29	07:00:02	44.8060	11.1030	17.1	5.8										
2012-05-29	08:15:10	44.8800	11.0290	16.6	4.3										
2012-05-29	08:25:50	44.7955	10.8797	17.8	4.4	b	X	X	X	X	X	X	X	X	X
2012-05-29	08:40:57	44.8297	10.8972	17.9	4.6	b	X	X	X	X	X	X	X	X	X
2012-05-29	09:01:34	44.9087	10.9963	13.3	3.7										
2012-05-29	09:14:08	44.8625	10.9453	13.7	3.6										
2012-05-29	09:24:32	44.7702	10.9860	17.7	3.6										
2012-05-29	09:30:22	44.8988	11.0560	13.8	4.0	a	X	X	X	X	X	X	X	X	X

Table 2 continued

Date	Time (UTC)	Lat (°)	Long (°)	Depth (km)	M	Ref. Figs. 3 and 4	OGO*							
							01	02	03	04	05	06	07	08
2012-05-29	10:55:55	44.7945	10.8882	14.0	5.5	d	X	X	X	X	X	X	X	X
2012-05-29	10:59:59	44.8395	10.8227	16.3	5.1	c	X	X	X	X	X	X	X	X
2012-05-29	11:07:05	44.9002	10.9738	14.0	4.1	a	X	X	X	X	X	X	X	X
2012-05-29	14:39:41	44.8845	10.9822	13.8	3.9	a	X	X	X	X	X	X	X	X
2012-05-29	18:28:04	44.8988	10.9123	17.5	3.8									
2012-05-29	18:44:41	44.8772	11.0038	10.1	3.6									
2012-05-30	06:00:34	44.8677	10.9697	17.1	3.9	a	X	X	X	X	X	X	X	X
2012-05-30	12:01:43	44.8637	11.1073	13.7	3.6									
2012-05-31	04:21:56	44.8628	11.1780	15.5	3.7									
2012-05-31	14:58:21	44.8518	10.8582	17.2	4.2									
2012-05-31	19:04:02	44.7868	10.9538	17.5	4.4	b	X	X	X	X	X	X	X	X
2012-06-01	12:22:44	44.8203	10.9910	17.6	3.7									
2012-06-03	17:57:53	44.9122	10.9783	16.2	3.8									
2012-06-03	19:20:42	44.7842	10.8355	16.1	5.1	c	X	X	X	X	X	X	X	X
2012-06-03	23:40:59	44.8895	10.9377	16.8	3.6									
2012-06-04	06:55:49	44.9373	11.0080	16.4	4.1	a	X	X	X	X	X	X	X	X
2012-06-06	04:08:33	44.4340	12.3540	25.6	4.5	b*	X	X	X	X	X	X	X	X
2012-06-12	01:48:36	44.9132	10.8923	16.8	4.4	b	X	X	X	X	X	X	X	X
2012-06-14	06:48:30	44.8495	10.9638	15.9	3.8									
2012-06-15	08:59:44	44.8532	11.1990	17.5	3.8									
2012-06-15	22:13:49	44.8783	11.1808	15.1	3.9	a	X	X	X	X	X	X	X	X

Letters a, b, c, and d refer to Figs. 3 and 4 where the events recorded by each station are marked by X

04:08:33 UTC, MI 4.5, Mw 4.1 (Saraò and Peruzza 2012). For this event, the preliminary locations published in the ISIDe database (<http://iside.rm.ingv.it>) were used because OGS station coverage is not optimal in this sector. This earthquake (hereafter called the Comacchio earthquake) does not belong to the Emilia sequence and was located offshore, at the easternmost edge of the plain, a few kilometers southeast of Comacchio Lagoon (Fig. 1) at a hypocentral depth of 25.6 km. Nucleation was established at a shallower 17 km for most of the earthquakes, with the exception of the Comacchio earthquake, whose hypocenter was located 25 km deep. The focal mechanisms were principally thrust, with some earthquakes showing a strike-slip mechanism (Saraò and Peruzza 2012).

The waveforms were checked visually to avoid biasing peaks coming from saturated signals, and records of the main event of May 29, 7:00:02 UTC, for four stations were rejected because analysis indicated saturation on all components.

3 Ground-motion parameters

PGA, PGV, and response spectra (SA) for all events shown in Table 2 were examined. The main shock on May 29, 7:00:02 UTC, was recorded by all stations in the OGS network, but amplitudes were saturated on four sites. Figure 2 shows the waveforms and the PGA values for this event for sites where the signals were not saturated.

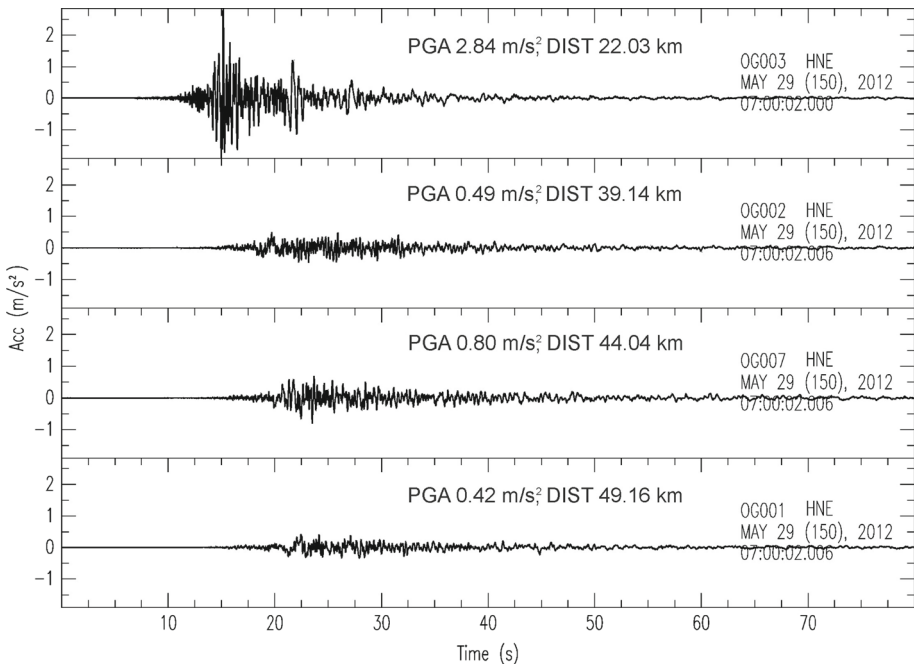


Fig. 2 Waveforms of the EW components of ground acceleration as recorded by the OGS temporary network and sorted by epicentral distance at those stations not saturated during the May 29, 7:00:02 UTC event. PGA (in m/s^2) and epicentral distances are given

The values obtained at the selected sites were compared with the ground-motion parameters estimated by BI11, assuming that all sites belonged to the C class (soft soils, $V_s < 360 \text{ m/s}$), in agreement with the EC8 provisions (ENV 1998, 2002) for a reverse fault mechanism. Epicentral distances were used in the analysis. PGA and PGV values of the vertical and the geometrical means of the two horizontal components were computed, and the acceleration response spectra for the horizontal components were calculated for the same 20 periods ranging between 0.04 and 2 sec by BI11.

Because the volume of records for all stations was large, details of the PGA/PGV values of one subset of the data are studied here. The dataset was divided into four classes of local magnitude: 4.0 ± 0.1 , 4.5 ± 0.1 , 5.1 ± 0.1 , and 5.5 ± 0.1 (Figs. 3 and 4). Table 2 gives the events in each class.

The observed PGA and PGV were fitted quite well by the BI11 estimates and followed the trend of the subset shown here, even though some values were dispersed, both higher and lower than predictions, and both for low magnitudes and higher. In particular, class 4.0 (Fig. 3a) had the largest number of events, including 11 earthquakes (five events with $ML = 4.1$, three events with $ML = 4.0$, and three events with $ML = 3.9$). In this class, all the events are equally spread along the predicted curve, within $\pm\sigma$, with few cases lower than predicted values. The OG004 site on the NS component recorded a strong PGA (and also PGV) value, higher than predictions, for the event of June 4, 6:55:49 UTC. This can be related to the source mechanism of the event that, according to moment-tensor inversion (Sarà and Peruzza 2012), was reverse with strike 273, dip 58, and rake 91, which could have increased the displacement in the NS direction at the OG004 site.

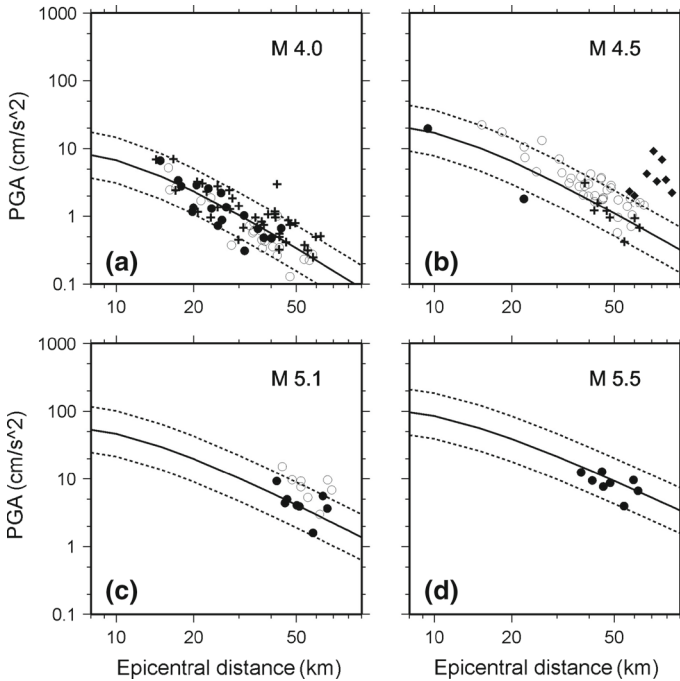


Fig. 3 a–d show the observed PGA values for events of various magnitude classes, as reported in Table 2, versus the BI11 empirical curve calculated for ML 4.0, 4.5, and 5.3 (solid and dashed lines represent the mean value and $\pm\sigma$). In (a), the black dots represent events of ML = 4.0, the white circles events of ML = 3.9, and the crosses events of ML = 4.1. In (b), the black dots are events of ML = 4.5, the white circles are events of ML = 4.4, and the crosses are the event of May 29, 8:40:57 UTC of ML = 4.6. The black diamonds represent the Comacchio event, ML = 4.5. In (c), the black dots represent the event of May 29, 10:59:59 UTC, and the white circles the event of June 3, 19:20:42 UTC, both of ML = 5.1. (d) The event of May 29, 10:55:55 UTC, ML = 5.5

Class 4.5 (Fig. 3b) contains eight events, including five earthquakes of magnitude 4.4, two events of magnitude 4.5, and one of magnitude 4.6. In this case, a good fit can be observed both for magnitude 4.4 and for 4.6. An exception is the Comacchio event, with observed PGA values three scale units higher than expected for those stations with an epicentral distance of about 70 km. Such a great discrepancy could be related to post-critically reflected S-waves and multiples from the Moho (SmSM). This particular case will be discussed in the following paragraph.

The two events in class 5.1 (Fig. 3c) are well fitted by the prediction law for the PGA, and the same holds for the single event in class 5.5 (Fig. 3d). More discrepancies arise in the PGV data (Fig. 4), not for class 4.0 (Fig. 4a), which is well constrained, but for class 4.5 (Fig. 4b) and for class 5.1 (Fig. 4c). Excluding the Comacchio event, in class 4.5, the higher values are related to the event on May 27, 18:18:44 UTC, which was, according to moment-tensor inversion (Saraò and Peruzza 2012), a strike-slip event. This fact could have influenced the closer sites that might not have been well constrained by the prediction law for reverse events. For class 5.1 (Fig. 4c), the event on June 3, 19:20:42 UTC, fitted the predictions quite well, while the event on May 29, 10:59:59 UTC, showed PGV values higher than predicted. This event, following by a few minutes the main event of May 29, 10:55:55 UTC, ML = 5.5, was characterized by source and propagation effects that are not taken into account by GMPE. The main event of class 5.5 (Fig. 4d) is underestimated for

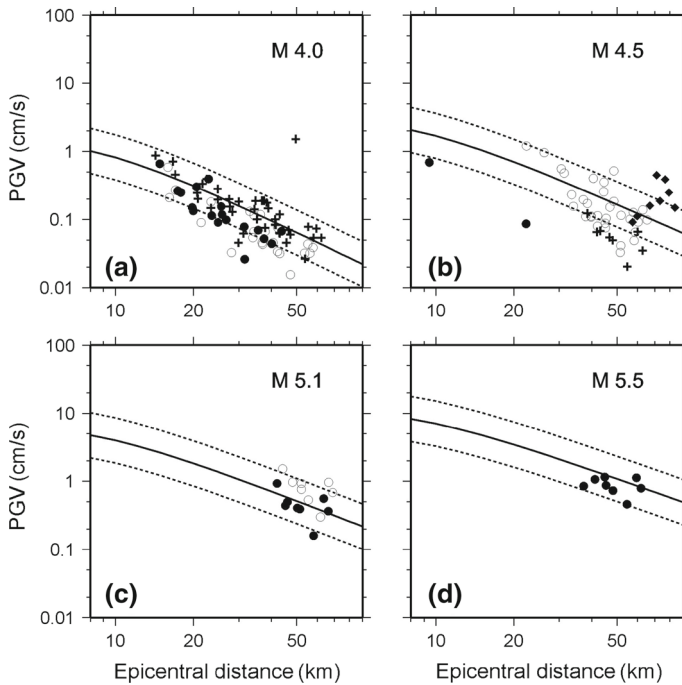


Fig. 4 The same as in Fig. 3, but for PGV

the more distant sites. This effect can be explained by the observation that the main events of the Emilia sequence were characterized by a considerable amount of elastic energy that was released as local surface waves which increased in amplitude with increasing epicentral distance (Bordoni et al. 2012).

The results for the acceleration-response spectra (SA) followed approximately the PGV trend, with some events underestimated by BI11 and others well fitted. In general, for larger events, the longer periods were underestimated by BI11. Bordoni et al. (2012) observed the same behavior for the main event of May 29, 2012, in the EMERSITO network in the epicentral area and attributed it to the low-frequency content of the horizontal ground motion, which was larger than the average trend expected for Italy because of the deep sediments of the Po Plain. Figure 5 shows the SA model of the event of May 29, 10:55:55 UTC, $M_L = 5.5$. In spite of a generally good fit between observed and predicted SA values, a number of values are on the edge of the upper standard deviation, and for the OG001 and OG007 sites, the two sites with larger epicentral distances, the measured data were higher for periods longer than 0.4–0.5 s, confirming the general trend.

4 The Comacchio earthquake

Figures 3, 4, and 6 illustrate that all parameters related to the Comacchio earthquake (Fig. 7) were considerably larger than the BI11 estimates; this behavior can be explained by S-wave reflections at the Moho boundary.

It has been observed that post-critically reflected S-waves and multiples from the Moho (SmSM) discontinuity can play an important role in ground motion due to medium to strong

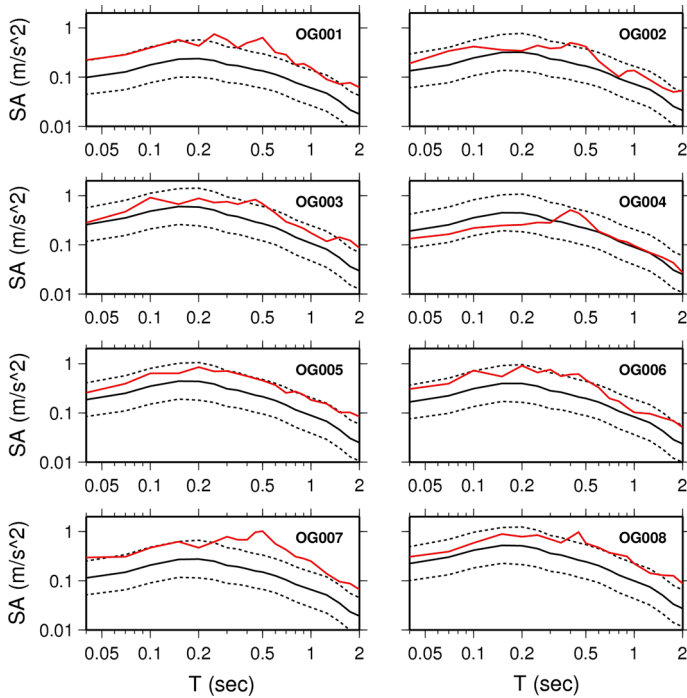


Fig. 5 Comparison of the geometric mean of the two horizontal components of the acceleration response spectra of the May 29, 10:55:55 UTC event, $M_L = 55$ (red line) with predictions from the equations of Bindi et al. 2011 (black solid line, SD in black dotted lines)

earthquakes away from the source (Bakun and Joyner 1984; Burger et al. 1987; Liu and Tsai 2009; Eberhart-Phillips et al. 2010; Bragato et al. 2011). Recently, some earthquakes from the 2012 Emilia seismic sequence have been used to investigate the SmSM domain and the corresponding spectral amplitude scaling with magnitude (Sugan and Vuan 2013).

Accelerometric data show that high-amplitude SmSM reflections can be recognized within the Po Plain and at the boundaries between the Po Plain and the Alpine Chain at epicentral distances greater than 80 km, in the frequency range from 0.25 to 3 s, and in the group velocity window from about 2.6 to 3.2 km/s. Using available regression relationships between macroseismic intensity and pseudo-spectral accelerations and Housner intensities, Sugan and Vuan (2013) found that a damage level due to SmSM can be reached in the far field, assuming a maximum credible earthquake in the Po Plain ($M_w = 6.7$).

The method described in Sugan and Vuan (2012) was applied to the dataset of the event occurring on June 6, 2012 (at 04:08:33 UTC), which was recorded by the temporary network to identify the possible SmSM amplitude enhancement domain. The procedure uses a single-station method for group-velocity period estimation based on the multiple-filter technique (MFT) and applied to accelerograms. Technical details of the analysis can be found in Sugan and Vuan (2012), where the method was validated using synthetic seismograms and observations. The data were corrected for instrument responses (velocigrams were differentiated to obtain accelerograms) and rotated to provide radial and transverse components. MFT was performed for each station, and the transverse and radial components in the group velocity and period ranged from 1 to 5 km/s and from 0.1 to 5 s respectively. The SmSM

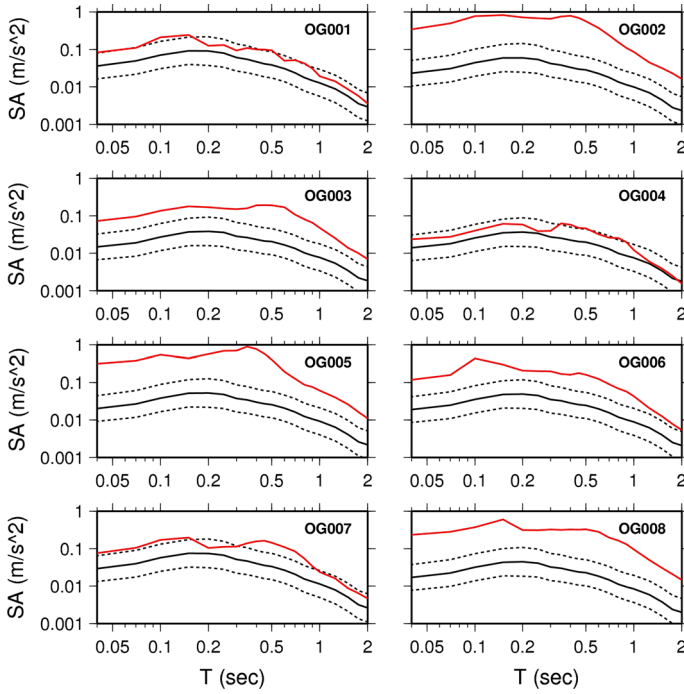


Fig. 6 The same as Fig. 5, but for the Comacchio event, $M=4.5$

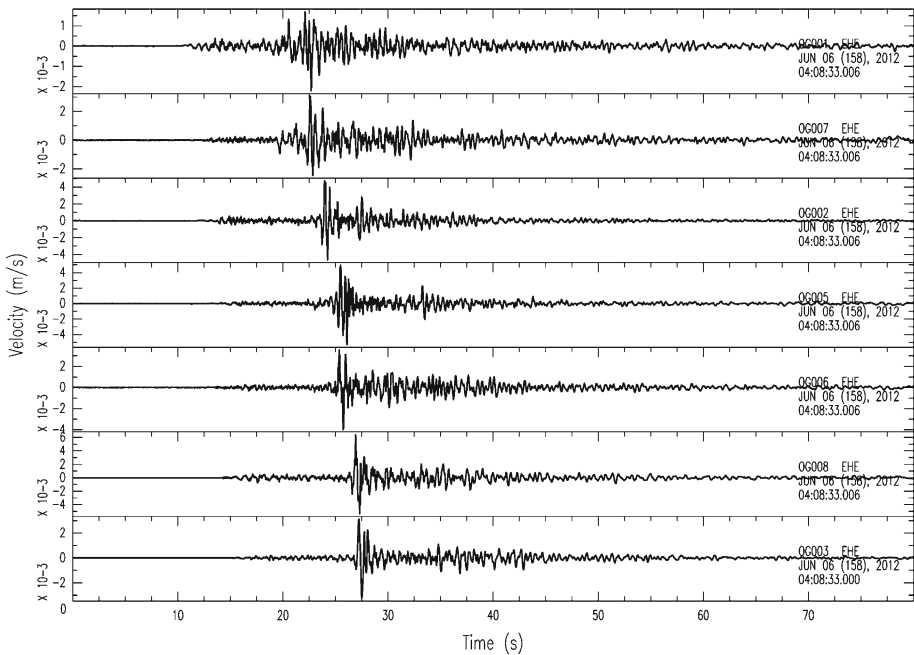


Fig. 7 Velocity EW components of the Comacchio event sorted by increasing epicentral distance

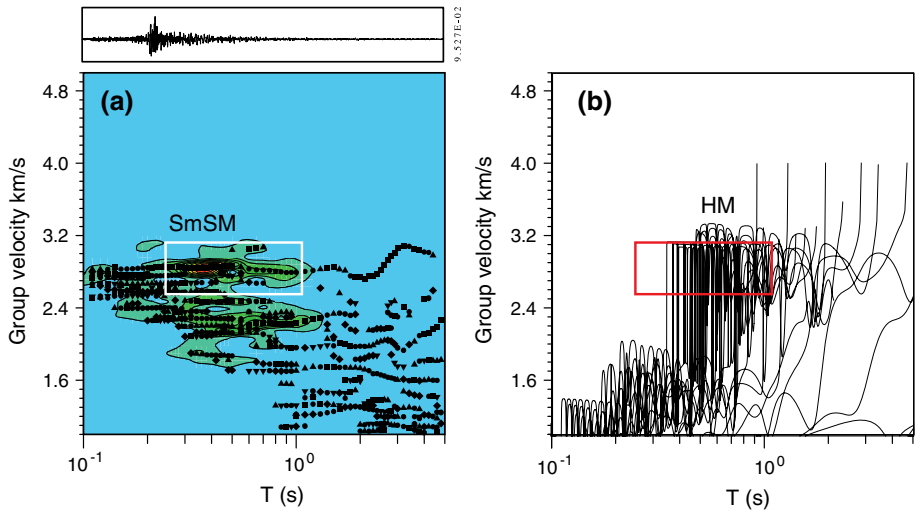


Fig. 8 **a** MFT analysis of the OG005 seismic station (radial component of the accelerogram is shown in the *inset*) and **b** theoretical Rayleigh wave dispersion curves from the velocity model proposed by Malagnini et al. (2012). The contoured color scale is in dB; red = 100 dB. Dotted black symbols show the maximum coherence of the signal. Black curves show the theoretical Rayleigh wave dispersion curves for the fundamental and the first 19 higher modes (HM) calculated according to Herrmann and Ammon (2002). The boxes highlight the SmSM as a superposition of the HM of surface waves along the same velocity waveguide. See Fig. 1 for station location

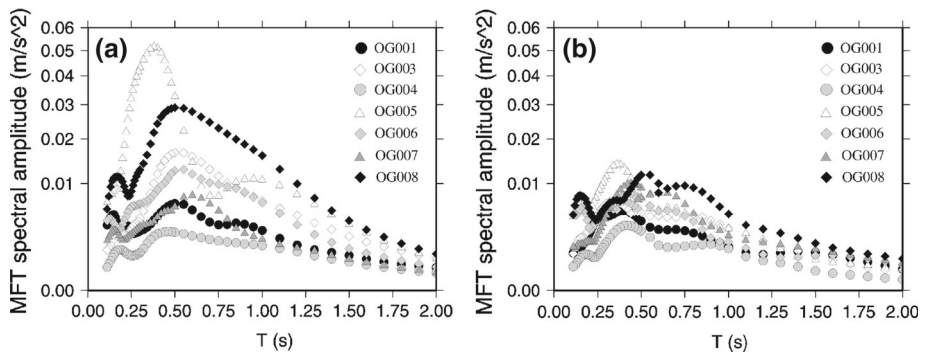


Fig. 9 MFT spectral amplitude-period graphs for the events occurring on June 6, 2012 (at 04:08:33 UTC), accelerometric (a) transverse and (b) radial components. See Fig. 1 for earthquake and station locations

can be clearly observed as a superposition of the higher modes of the surface waves (Oliver and Ewing 1957, 1958) along the same velocity waveguide, in the period range of 0.25–1 s and the velocity range of 2.8–3.2 km/s (Fig. 8). These observations are in agreement with Suga and Yuan (2013). On the basis of MFT analysis, the amplitude period graphs for the stations of the temporary network located at an epicentral distance from about 66 to 93 km could be represented. Almost all the stations show two peaks (Fig. 9): the first is related to the arrival of S-waves (periods less than 0.25 s) and the second, characterized by a greater spectral amplitude, to the arrival of SmSM reflections (periods up to 1–2 s). The major SmSM spectral amplitudes can be observed for the transverse component of the OG005 and OG008 seismic stations at periods from 0.25 to 1 s.

The observed SmSM spectral amplitude was enhanced by certain site effects that characterized the various stations in the temporary network (Priolo et al. 2012), and the relatively lower periods of SmSM reflections recorded at the surface are well correlated with the soft soil type. In general, for soft soils, moving from borehole to surface, the SmSM maximum spectral amplitude along a given velocity waveguide moves toward lower periods for higher modes (Sugan and Vuan 2012). In the SmSM frequency range considered in this study, Cocco et al. (2001) indicated a possible amplitude enhancement of approximately six times from borehole to surface.

5 Discussion and conclusions

Strong-motion parameters (PGA, PGV, and spectral acceleration) at the sites of the OGS temporary network deployed in the Ferrara area the day after the main shock of May, 20, 2012, have been analyzed. The OGS Archive System of Instrumental Seismology (OASIS; <http://oasis.crs.inogs.it>) has collected all the data and station information under network code ZR. Access to the data is free, and any piece of waveform can be downloaded for further investigation. In this research, the authors' observations were compared with the values predicted by the ground-motion equations developed by Bindi et al. (2011). Assumptions were the geometric mean of horizontal components, a reverse fault mechanism, and that all the stations belonged to a soft-soil classification (class C, $V_s < 360$ m/s). This study considered 46 earthquakes in the range magnitude of 3.6–5.5 and for distances up to 90 km. The main event of May 29, 07:00:02 UTC, $M_L = 5.8$, created saturation at four sites of the array.

From the dataset used, the PGA observed values are in good agreement with the predictions of the attenuation law. More discrepancies arise for the PGV observations. Low-magnitude events are well predicted or only slightly overestimated, while for larger magnitudes and increasing epicentral distances the predictions underestimated the observations. This observation could be explained by the large amount of elastic energy released as surface waves due to the strong impedance contrast between soft alluvial cover and bedrock. The main events of the Emilia sequence are characterized by a large quantity of low frequencies that are not well predicted by the present GMPE because of the lack of records in the Po Plain.

A peculiar behavior was shown by the event occurring on June 6, 04:08:33 UTC, on the easternmost edge of the plain, a few kilometers east of Comacchio Lagoon at a depth of 25 km. This event, $M_L = 4.5$, showed PGA values that exceeded the GMPE by three times for stations distant more than 70 km. Using time-frequency analysis, it could be suggested that the observed PGA values for this event were due to SmSM reflections, enhanced by the site effects that characterized the stations of the temporary network, which were located on soft soils (Cocco et al. 2001; Priolo et al. 2012). Moreover, in this case, the great discrepancy with respect to GMPE is related to the hypocentral depth of the event, which brought it quite close to the Moho boundary.

Acknowledgments This research has been supported by the Dipartimento della Protezione Civile: Project S2, ProCiv-INGV (2012–2013). We thank Angela Saraò and Pier Luigi Bragato, who gave us much support and many suggestions and two anonymous reviewers to improve the manuscript.

References

- Bakun WH, Joyner WB (1984) The ml scale in central california. *Bull Seismol Soc Am* 74(5):1827–1843
- Bindi D, Pacor F, Luzi L, Puglia R, Massa M, Ameri G, Paolucci R (2011) Ground-motion prediction equations derived from the italian strong motion database. *Bull Earthq Eng* 9:1899–1920

- Bordoni P, Azzara RA, Cara F, Cogliano R, Cultrera G, Di Giulio G, Fodarella A, Milana G, Pucillo S, Riccio G, Rovelli A, Puglia R, Ameri G (2012) Preliminary results from EMERSITO, a rapid response network for site-effect studies. *Ann Geophys* 55. doi:[10.4401/ag-6153](https://doi.org/10.4401/ag-6153)
- Bragato PL, Sugan M, Augliera P, Massa M, Vuan A, Sarà A (2011) Moho reflection effects in the Po plain (northern Italy) observed from instrumental and intensity data. *Bull Seismol Soc Am* 101(5):2142–2152. doi:[10.1785/0120100257](https://doi.org/10.1785/0120100257)
- Burger RW, Somerville PG, Barker JS, Herrmann RB, Helmberger DV (1987) The effect of crustal structure on strong ground motion attenuation relations in eastern north america. *Bull Seismol Soc Am* 77(2):420–439
- Castelli V, Bernardini F, Camassi R, Caracciolo CH, Ercolani E, Postpischl L (2012) Looking for missing earthquake traces in the Ferrara-Modena plain: an update on historical seismicity *Ann Geophys* 55. doi:[10.4401/ag-6110](https://doi.org/10.4401/ag-6110)
- Cocco M, Ardizzoni F, Azzara RM, Dall'Olivo L, Delladio A, Di Bona M, Malagnini L, Margheriti L, Nardi A (2001) Broadband waveforms and site effects at a borehole seismometer in the Po alluvial basin (Italy). *Ann Geophys* 44:137–154
- Eberhart-Phillips D, McVerry G, Reyners M (2010) Influence of the 3d distribution of q and crustal structure on ground motions from the 2003 Mw 7.2 Fiordland New Zealand earthquake. *Bull Seismol Soc Am* 100(3):1225–1240
- Fantoni R, Franciosi R (2010) Tectono-sedimentary setting of the Po Plain and Adriatic foreland. *Rend Fis Acc Lincei* 21(1):S197–S209. doi:[10.1007/s12210-010-0102-4](https://doi.org/10.1007/s12210-010-0102-4)
- Herrmann RB, Ammon CJ (2002) *Computer Programs in Seismology*, Version 330. Saint Louis University, St Louis, Missouri, http://www.eas.slu.edu/eqc/eqc_cps/CPS/CPS330/cps330cpdf
- Liu KS, Tsai YB (2009) Large effects of Moho reflections (smsm) on peak ground motion in northwestern Taiwan. *Bull Seismol Soc Am* 99(1):255–267
- Malagnini L, Herrmann RB, Munafò I, Buttinelli M, Anselmi M, Akinci A, Boschi E (2012) The 2012 Ferrara seismic sequence: regional crustal structure earthquake sources and seismic hazard. *Geophys Res Lett*. doi:[10.1029/2012GL053214](https://doi.org/10.1029/2012GL053214)
- Martelli L, Severi P, Biavati G, Rosselli S, Camassi R, Ercolani, Marcellini A, Tenta A, Gerosa D, Albarello D, Guerrini F, Lunedei, Pileggi D, Pergalani F, Compagnoni M, Fioravante V, Giretti D (2011) Analysis of the local seismic hazard for the stability tests of the main bank of the Po River. Gruppo Nazionale di Geofisica della Terra Solida (GNGTS), 30° Convegno Nazionale, Trieste, pp 14–17 November 2011
- Meletti C, D'Amico V, Ameri G, Rovida A, Stucchi M (2012) Seismic hazard in the Po Plain and the 2012 Emilia earthquakes. *Ann Geophys* 55. doi:[10.4401/ag-6158](https://doi.org/10.4401/ag-6158)
- Norme Tecniche per le Costruzioni, (NTC) (2008) *Norme Tecniche per le Costruzioni*. Ministerial Decree 14/01/2008/, Official, Gazette no. 29, February 4, 2008
- OGS, 2013 *Bollettino della Rete Sismometrica del Friuli Venezia Giulia CRS*, Udine, Italy, <http://www.crsinogsit/bollettino/RSFVG>, last accessed March 2013
- Oliver J, Ewing M (1957) Higher modes of continental Rayleigh waves. *Bull Seismol Soc Am* 47:187–204
- Oliver J, Ewing M (1958) Normal modes of continental surface waves. *Bull Seismol Soc Am* 48:33–49
- Pacor F, Paolucci R, Luzi L, Sabetta F, Spinelli A, Gorini A, Nicoletti M, Marcucci S, Filippi L, Dolce M (2011) Overview of the Italian strong-motion database itaca 1.0. *Bull Earthq Eng* 9:1723–1739
- Priolo E, Romanelli M, Barnaba C, Mucciarelli M, Laurenzano G, Dall'Olivo L, Abu-Zeid N, Caputo R, Santarato G, Vignola L, Lizza C, Di Bartolomeo P (2012) The Ferrara thrust earthquakes of May–June 2012: preliminary site response analysis at the sites of the OGS temporary network. *Ann Geophys* 55. doi:[10.4401/ag-6172](https://doi.org/10.4401/ag-6172)
- Rovida A, Camassi R, Gasperini P, Stucchi M (eds.) (2011) CPTI11, the 2011 version of the Parametric Catalogue of Italian Earthquakes. Milano, Bologna, <http://emidius.mi.ingv.it/CPTI11>. doi:[10.6092/ingv.it-cpti11](https://doi.org/10.6092/ingv.it-cpti11)
- Sarà A, Peruzza L (2012) Fault plane solutions from moment tensor inversion and preliminary Coulomb stress analysis in the Emilia Plain. *Ann Geophys* 55. doi:[10.4401/ag-6134](https://doi.org/10.4401/ag-6134)
- Scognamiglio L, Margheriti L, Mele F, Tinti E, Bono A, De Gori P, Lauciani V, Lucente FP, Mandiello AG, Marocci C, Mazza S, Pintore S, Quintiliani M (2012) The 2012 Pianura Padana Emiliana seismic sequence: locations and magnitudes. *Ann Geophys* 55. doi:[10.4401/ag-6159](https://doi.org/10.4401/ag-6159)
- Stucchi M, Meletti C, Montaldo V, Crowley H, Calvi GM, Boschi E (2011) Seismic hazard assessment (2003–2009) for the Italian building code. *Bull Seismol Soc Am* 101:1885–1911. doi:[10.1785/0120100130](https://doi.org/10.1785/0120100130)
- Sugan M, Vuan A (2012) Evaluating the relevance of Moho reflections in accelerometric data: application to an inland Japanese earthquake. *Bull Seismol Soc Am* 102(2):842–847. doi:[10.1785/0120110085](https://doi.org/10.1785/0120110085)
- Sugan M, Vuan A (2013) On the ability of Moho reflections to affect the ground motion in northeastern Italy: a case study of the 2012 Emilia seismic sequence. *Bull Earthquake Eng*. doi:[10.1007/s10518-013-9564-y](https://doi.org/10.1007/s10518-013-9564-y)

Tertulliani A, Arcoraci L, Berardi M, Bernardini F, Brizuela B, Castellano C, Del Mese S, Ercolani E, Graziani L, Maramai A, Rossi A, Sbarra M, Vecchi M (2012) The Emilia 2012 sequence: a macroseismic survey. *Ann Geophys* 55. doi:[10.4401/ag-6140](https://doi.org/10.4401/ag-6140)